Journal of Porphyrins and Phthalocyanines
J. Porphyrins Phthalocyanines 2014; **18**: 290–296
DOI: 10.1142/S1088424614500011

Catalytic activity to lithium-thionylchloride battery of different transitional metal carboxylporphyrins

Xiangfei Lü[a,b], Nan jiang Hu[c], Jun Li[a*], Zeng qi Zhang[a] and Wei Tang[c]

[a] *Key Laboratory of Synthetic and Natural Functional Molecule Chemistry of Ministry of Education, College of Chemistry & Materials Science, Northwest University, Xi'an, Shaanxi 710069, PR China*
[b] *Department of Environmental Engineering, College of Resource and Environment Science, Shaanxi University of Science and Technology, Xi'an, Shaanxi 710021, PR China*
[c] *Department of Process Equipment Control and Engineering, College of Light Industry and Energy, Shaanxi University of Science and Technology, Xi'an, Shaanxi 710021, PR China*

Received 22 October 2013
Accepted 14 December 2013

ABSTRACT: The 5-(4-carboxylatomethoxy)phenyl-10,15,20-triphenyl porphyrin (H_2Pp) and its transition metal complex (MPp, M = Zn^{2+}, Co^{2+}, Ni^{2+}, Cu^{2+}) were synthesized and characterized by IR, UV-vis, MS and elementary analysis. Electrocatalytic effects associated with the reduction of thionyl chloride in a lithium/thionyl chloride ($Li/SOCl_2$) battery containing H_2Pp and its transition metal complex (MPp, M = Zn^{2+}, Co^{2+}, Ni^{2+}, Cu^{2+}) are evaluated by the relative energy of the battery and discharge time. The results indicate that the energy of $Li/SOCl_2$ battery catalyzed by CuPp and ZnPp is 103.7%, 106.3%, respectively, higher than that of $Li/SOCl_2$ battery in the absence of the porphyrins. The energy of $Li/SOCl_2$ battery whose electrolyte contains NiPp and CoPp is similar to that of the cell in the absence of these complexes. It shows that the electronic configuration of the central metal ion influences a charge-transfer process during the reduction of thionyl chloride. With the increasing numbers of d electrons of the central metal ion, the catalytic activity of MPps was enhanced. The ZnPp with electronic configuration d^{10} of central metal ion exhibits relatively high catalytic activity.

KEYWORDS: transition metal carboxylporphyrin, lithium-thionylchloride battery, electrochemical properties.

INTRODUCTION

There is an urgent need for developing efficient catalyst for lithium-thionylchloride battery since it is one of the best primary batteries [1–3]. In spite of lithium-thionylchloride battery with high discharge voltage and energy density, its energy in practice that is much lower than in the theory is still one of limitations [4]. That is because the system consists of Li anode, a carbon cathode and a $LiAlO_4$-$SOCl_2$ electrolyte, and the Li anode is prevented from reacting with $SOCl_2$ *via* the formation of LiCl passivation film and sulfur. The considerable research efforts in the field of catalysis for $Li/SOCl_2$ battery have been done to promote the practical energy of $Li/SOCl_2$ battery [5–8].

One possible approach to enhance the cell performance is the addition of catalyst molecules which must be readily oxidizable/reducible and accelerate the rate of electron transfer. Among these works, using macromolecular compounds, especially metal phthalocyanine (MPc) compounds acting as catalyst attracted considerable interest [9–11]. Choi and co-workers reported on some Schiff base transitional metal compounds shows sizeable catalytic activity for the reduction of thionyl chloride [12]. Xu *et al*., after comparing different transition metal phthalocyanine, found the electronic configuration of the central metal ion strongly influences the catalytic activity of metal phthalocyanine to $Li/SOCl_2$ battery. They also predicted that the MPc derivatives whose central

---

*Correspondence to: Jun Li, email: junli@nwu.edu.cn, tel: +86 298-830-2604, fax: +86 298-830-3798 metal ions, such as Zn^{2+}, of electronic configuration d^{10}, exhibit excellent catalytic activity to $Li/SOCl_2$ battery [13, 14]. However, MPc derivatives were difficult to be purified during the preparation, which would reduce the catalysis in the $Li/SOCl_2$ battery.

Considering porphyrin derivatives have similar structure of phthalocyanine derivatives, high conjugated structure, good thermal stability, excellent electron conductivity and better solubility [15, 16]. Metal porphyrins are much more environmental compatible compared with metal phthalocyanines. The role of acidic functionality is important for the process, as it could enhance the catalytic activity of metal porphyrin in our several repeated experiments. The solubility of carboxylporphyrin may be better than that of the porphyrins containing non-polar groups in thionyl chloride which showed stronger adsorption to carboxyl group [17]. In addition, it has been demonstrated that carboxyl is easy to promote the formation of **$MPp\cdot SOCl_2$** due to the lager π elongation with low symmetry of carboxylporphyrin [18]. There are, however, few works discussed or analyzed the factors that affect the catalytic activity of the system in depth. In fact, several factors have been proved to influence the catalytic activity, including the center metal, the peripheral substituents of porphyrin molecules and axial ligand [19, 20]. In this paper, catalytic effects relative to thionyl chloride reduction were examined by evaluating the relative energy and discharge time in $Li/SOCl_2$ solution which contained different metal carboxylporphyrins. In order to better define the influence of different central metal ions, we focus on the analysis of the electronic configuration of the central metal ion in the catalytic activity of the metal carboxylporphyrin compounds.

EXPERIMENTAL

Reagents and materials

The relative energy of $Li/SOCl_2$ battery was used to evaluate the catalytic activity of the complexes. $LiAlCl_4/SOCl_2$ electrolyte (the concentration of $LiAlCl_4$ is 1.47 M), lithium pieces and carbon films were provided by Xi'an Institute of Electromechanical Information Technology, and other reagents were purchased from Tian Jin Chemical Reagents Company. All solvents and reagents were used without further purification except pyrrole was distilled before using. 5-(4-carboxylatomethoxy)phenyl-10,15,20-triphenyl porphyrin **(H_2Pp)** and metal porphyrins **(MPp)** (M = Zn^{2+}, Co^{2+}, Ni^{2+}, Cu^{2+}) were synthesized according to literature [21]. All chromatographic separations were carried out on silica gel (180–200 meshes).

Equipment

Elemental analysis (C, H and N) was performed by Vario EL-III CHNOS instrument. FT-IR spectra were registered in KBr using a BEQ UZNDX-550. UV-vis spectra were recorded by a Shimadzu UV-vis-NIR spectrophotometer (UV-3100). Mass spectrometry analysis was carried out on a matrix assisted laser desorption/ionization time of flight mass spectrometer (MALDI-TOF MS, Krato Analytical Company of Shimadzu Biotech, Manchester, Britain) using a standard procedure involving 1 mL of the sample solution.

Synthesis of porphyrin and metal(II) porphyrins

Synthetic routes to porphyrin **(H_2Pp)** and metal porphyrins **(MPp)** are shown in Scheme 1 and the detailed synthetic procedures were as follows:

General procedure for the synthesis of carboxylporphyrin (H_2Pp). According to the method reported previously [21], 5-(4-carboxylatomethoxy)phenyl-10,15,-20-triphenyl porphyrin was synthesized by carrying out the hydrolysis of 5-(4-ethylacetatatomethoxy)phenyl-10,15,20-triphenyl porphyrin. **H_2Pp.** Yield 64%. mp: 250 °C (decomposed). Anal. calcd. for $C_{46}H_{32}N_4O_3$%: C, 80.21; H, 4.68; N, 8.13%. Found C, 80.15; H, 4.73; N, 8.09%. UV-vis ($CHCl_3$): λ_{max}, nm 419, 516, 551, 591, 645. FT-IR (KBr): ν, cm^{-1} 3437, 2925, 2731, 2362, 1695, 1631, 1398, 1259, 1103, 1037, 966, 806, 680. MS (FAB): *m/z* 689.66 (calcd. for $[M+H]^+$ 689.66).

General procedure for the synthesis of MPp (M = Zn^{2+}, Co^{2+}, Ni^{2+}, Cu^{2+}). 27.0 mg (0.15 mmol) of $M(CH_3COO)_2$ (M = Zn^{2+}, Co^{2+}, Ni^{2+}, Cu^{2+}) was added to 0.05 mmol of the **H_2Pp** dissolved in 20 mL $CHCl_3$ and 5 mL C_2H_5OH. The mixture was stirred for 24 h at 60 °C and monitored by TCL until the complete disappearance of the starting material **H_2Pp**. The unreacted solid salt was filtered and the solvent was removed under vacuum. The crude product was purified by chromatography on a silica gel column with $CHCl_3$ and CH_3COOH as eluent. **CuPp.** Yield 92%, mp 250 °C (decomposed). Anal. calcd. for $C_{46}H_{30}CuN_4O_3$: C, 73.64; H, 4.03; N, 7.47%. Found C, 73.67; H, 4.06; N 7.51%. UV-vis ($CHCl_3$): λ_{max}, nm

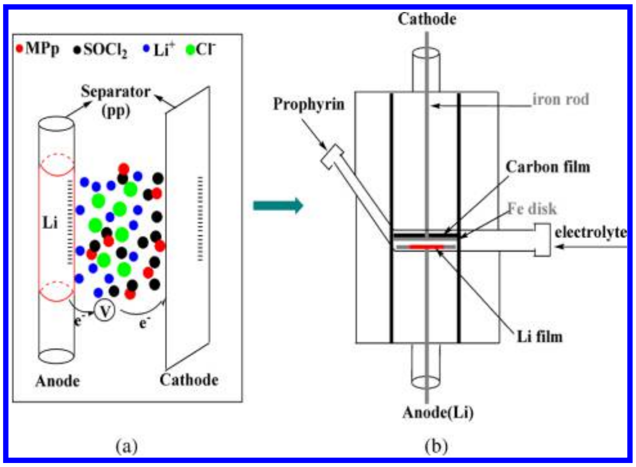

Fig. 1. The structure diagram (a) and mode (b) of $Li/SOCl_2$ battery

416, 540, 575. FT-IR (KBr): ν, cm^{-1} 3448, 2964, 2925, 1726, 1633, 1500, 1433, 1340, 1261, 1211, 1170, 1095, 1028, 802, 748, 703. MS (FAB): *m/z* 749.75 (calcd. for $[M + H]^+$ 749.75). **ZnPp.** Yield 95%; mp 250 °C (decomposed). Anal. calcd. for $C_{46}H_{30}ZnN_4O_3$: C, 73.46; H, 4.02; N, 7.45%. Found C, 73.50; H, 4.06; N, 7.47%. UV-vis ($CHCl_3$): λ_{max}, nm 421, 547, 585. FT-IR (KBr): ν, cm^{-1} 3450, 2962, 2850, 1631, 1485, 1431, 1336, 1363, 1213, 1174, 1070, 999, 800, 752, 700. MS (FAB): *m/z* 751.82 (calcd. for $[M + H]^+$ 750.16). **CoPp.** Yield 93%; mp 250 °C (decomposed). Anal. calcd. for $C_{46}H_{30}CoN_4O_3$: C, 74.09; H, 4.06; N, 7.51%. Found C, 74.07; H, 4.09; N, 7.47%. UV-vis ($CHCl_3$): λ_{max}, nm 419, 541, 573. FT-IR (KBr): ν, cm^{-1} 3728, 3444, 2925, 1631, 1409, 1080, 800, 675. MS (FAB): *m/z* 746.12 (calcd. for $[M + H]^+$ 746.16). **NiPp.** Yield 95%; mp 250°C (decomposed). Anal. calcd. for $C_{46}H_{30}NiN_4O_3$: C, 74.12; H, 4.06. Found C, 74.19; H, 4.02; N, 7.47%. UV-vis ($CHCl_3$): λ_{max}, nm 416, 539, 575. FT-IR (KBr): ν, cm^{-1} 3450, 2925, 1712, 1649, 1631, 1502, 1434, 1346, 1265, 1076, 1008, 800, 748, 696. MS (FAB): *m/z* 745.79 (calcd. for $[M + H]^+$ 745.17).

Electrochemistry

Electrochemical measurements were carried out in specially designed test cells. The compartment of the cells is made from PTFE material. Carbon films were used as cathode with the superficial area of 1 cm^2, and lithium pieces were used as the counter electrodes. 1 mL $LiAlCl_4/SOCl_2$ electrolyte solution containing 2 mg metal carboxylporphyrins was utilized. The discharge tests for the $Li/SOCl_2$ batteries were evaluated at a constant resistance 40 Ω, and were stopped when the voltage reached 2 V. All the experiments were implemented in a glove box under an argon atmosphere (MBRAUN, MB-BL-01). The structure diagram and mode of $Li/SOCl_2$ battery is shown in Fig. 1.

RESULTS AND DISCUSSION

Synthesis of the porphyrins

The synthetic route of the porphyrins and corresponding metal(II) carboxylporphyrins is illustrated in Scheme 1. The insertion of metal ion into the porphyrin ring occurs by reacting the metal-free porphyrin with excess hydrated $M(CH_3COO)_2$ ($M = Zn^{2+}, Co^{2+}, Ni^{2+}, Cu^{2+}$) in the mixed solvents of chloroform and acetic acid under 60 °C.

The UV-vis spectra of H_2Pp and MPps is shown in Fig. 2. The UV-vis spectra of different MPps were

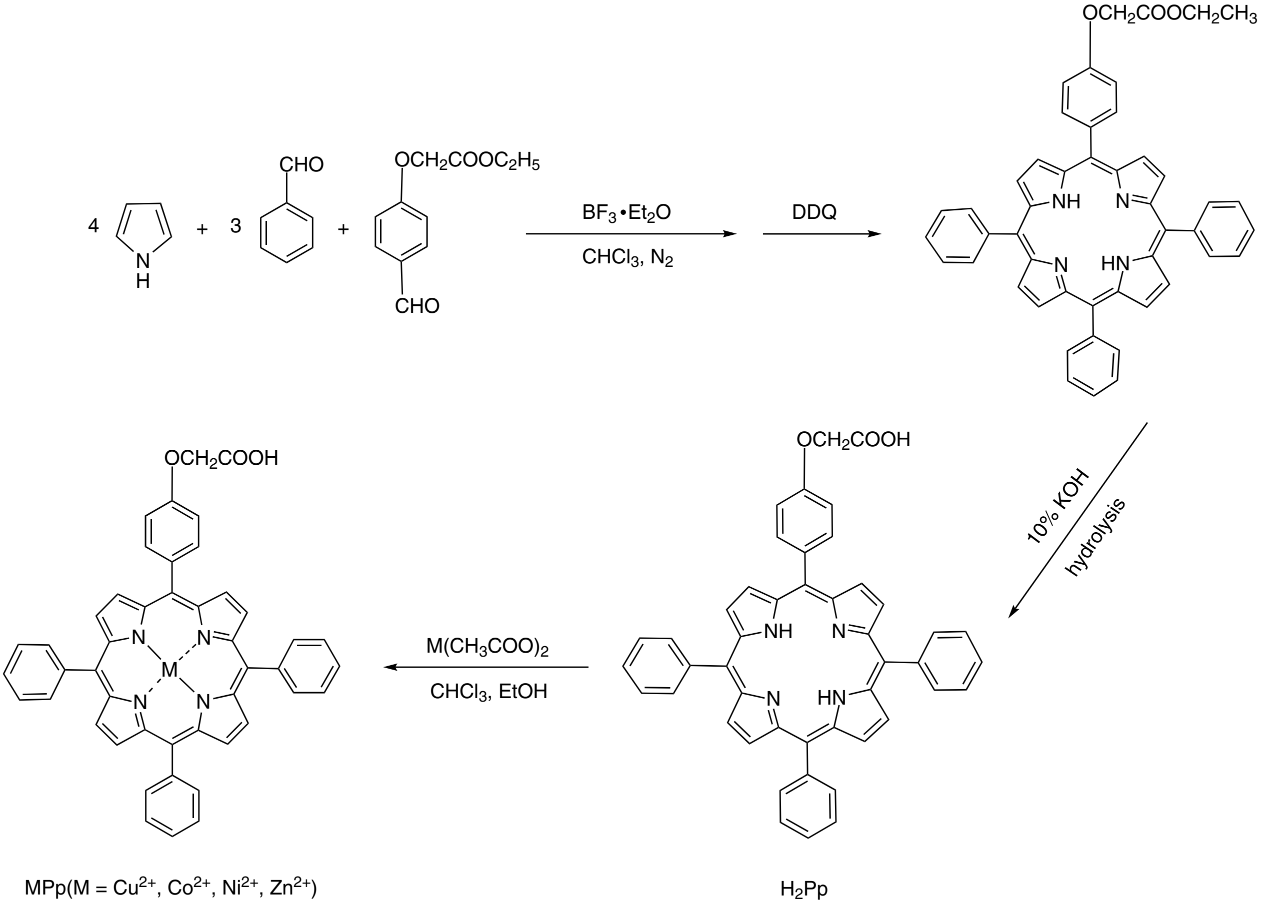

Scheme 1. Synthesis routes of the porphyrins

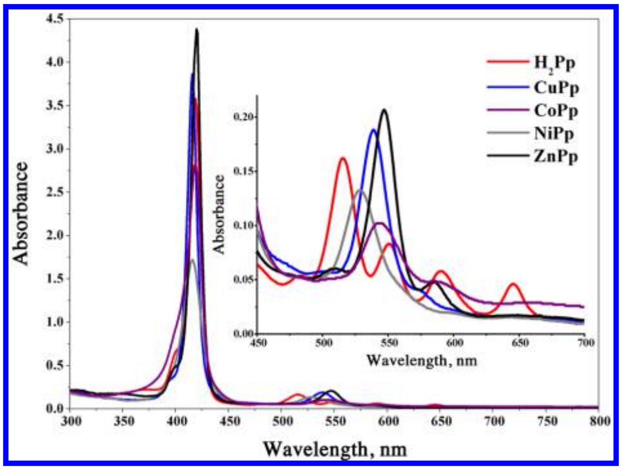

Fig. 2. UV-vis spectra of MPp (M = H_2, Cu^{2+}, Co^{2+}, Ni^{2+}, Zn^{2+}) 1×10^{-4} M ($CHCl_3$)

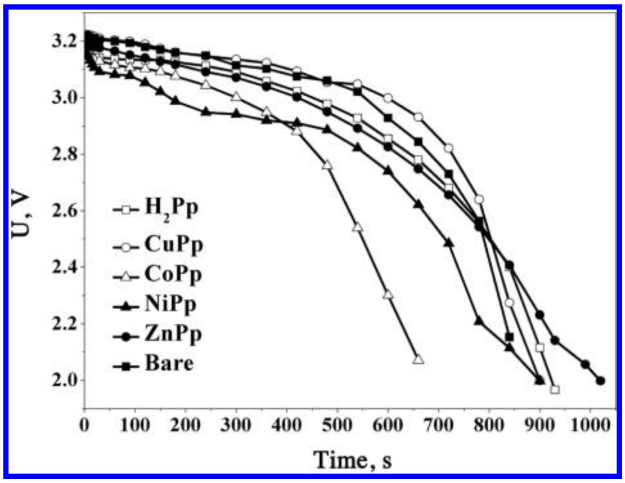

Fig. 3. The discharge curves of the Li/$SOCl_2$ battery

investigated to show the electron transitions between highest occupied molecular orbital (HOMO) and the lowest orbital molecular orbital (LUMO) of the metal carboxylporphyrins. The insertion of metal(II) into the porphyrin ring caused a violet shift of the corresponding Soret bands and Q-band for UV-vis spectra, as well as a decreasing number of Q-bands, due to the symmetry of the porphyrin ring increases when the H ions of N–H are replaced by metal(II). There are a relatively strong B-band and a weak Q-band existing in the electron absorbance of MPp. To MPp, the stronger band in the wavelength region of 410–420 nm ascribed to the π–π transition centred on the macrocycle of porphyrin ring is the Soret band. The UV-vis spectrum of MPp shows one Q-band at 529–547 nm, representing the characteristic band of different metal porphyrins. Compared to the free carboxylporphyrin, the absorption of MPps indicated different degree of red shift on Q-band. The Q-band of ZnPp is at 547 nm, much longer than that of other MPps, which may be benefit to the reduction of **MPp·SOCl$_2$**.

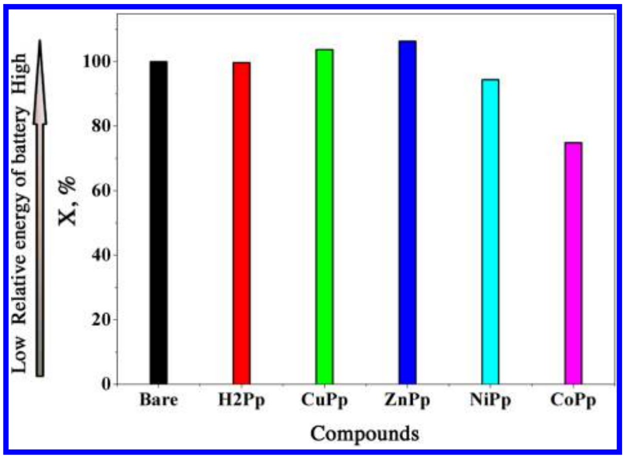

Fig. 4. Relative energy of Li/$SOCl_2$ battery catalyzed by the metal-free porphyrins

Table 1. The energy data of Li/$SOCl_2$ battery catalyzed by the metal-free porphyrins

Catalyst	U_{av}, V	C
blank	2.945	192.7
H_2Pp	2.856	192.1
CuPp	2.995	199.8
ZnPp	2.813	204.8
NiPp	2.776	181.9
CoPp	2.810	144.4

Mass spectroscopy data of **MPps** perfectly correspond to the expected $[M + H]^+$ m/z values. The principal change in the FI-IR spectra of metal(II) porphyrins compared with metal-free porphyrins is also the disappearance of stretching vibration of N–H.

Catalytic activity

The discharge curves of Li/$SOCl_2$ battery catalyzed by different MPps are shown in Fig. 3. It shows that the catalytic activity of MPp is different, depending on the metal ions. The battery's discharge time is 15 min for **CuPp**, 17 min for **ZnPp**, 15 min for **NiPp**, 11 min for **CoPp** and 15.5 min for **H$_2$Pp**. And the discharge time of Li/$SOCl_2$ battery catalyzed by metal phthalocyanines is lengthened 6–12 min [15]. It is indicated that the catalytic activity of the metal-porphyrins to Li/$SOCl_2$ battery is higher than that of metal phthalocyanines, when the central metal ion is same. In order to explain the catalytic activity of the compounds to Li/$SOCl_2$ battery, the relative energy of Li/$SOCl_2$ battery was calculated as follows:

The average discharge voltage of Li/$SOCl_2$ battery is:

$$U_{av} = \frac{\sum U\Delta t}{\sum \Delta t} \tag{1}$$

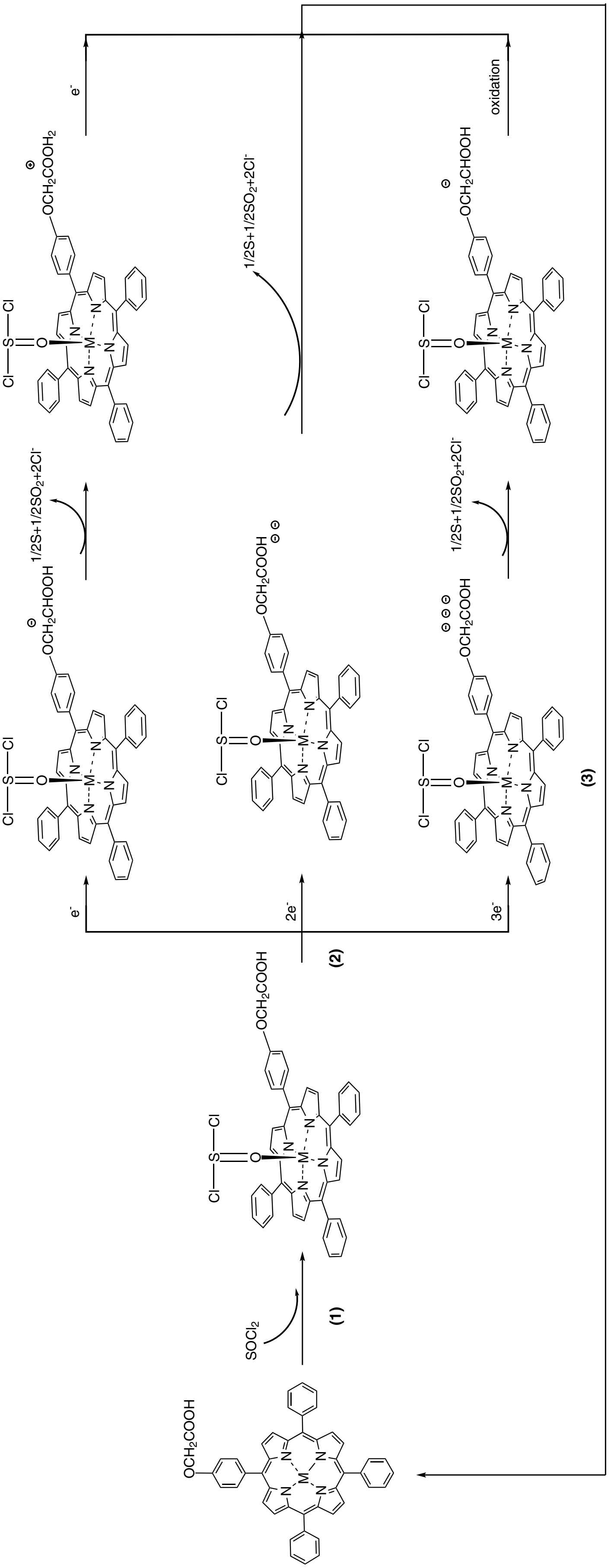

Fig. 5. The possible routes of the reduction of $SOCl_2$ catalyzed by MPp

The energy of Li/SOCl$_2$ battery is:

$$C = \int P dt = \int \frac{U^2}{R_e} dt = \sum \frac{U^2}{R_e} \Delta t = \frac{1}{R_e} \sum U^2 \Delta t = \frac{1}{40} \sum U^2 \Delta t \qquad (2)$$

where P is the discharge power of the battery, R_e is the constant resistance, U is the voltage discharged in the test.

The relative energy of the battery is:

$$X(\%) = \frac{C}{C_0} \times 100 \qquad (3)$$

where C stands for the energy of the battery, C_0 stands for the energy of the battery in the absence of complexes.

The energy of Li/SOCl$_2$ battery whose electrolyte contains **CuPp** and **ZnPp** is approximately 103–106% higher than that of the cell in the absence of complexes. By contrast with three kinds of compounds above, **H$_2$Pp**, **NiPp** and **CoPp** are inactive, and the energy of the Li/SOCl$_2$ battery whose electrolyte contains them is similar to that of the cell in the absence of complexes. The results indicate that the electronic configuration of metal ions ($[M]^{2+}$) is the key factor affecting the catalytic activity of the compounds in Li/SOCl$_2$ battery.

The relative energy(X) of Li/SOCl$_2$ battery reflects the catalytic activity of **MPp** clearly (as shown in Fig. 4). It shows that the relative energy of Li/SOCl$_2$ battery catalyzed by CuPp and ZnPp is 103.7%, 106.3% higher, respectively, than that of Li/SOCl$_2$ battery in the absence of complexes. These consequences are also listed in the Table 1. Furthermore, this conclusion is well consistent with the previous results of discharge curves.

During the discharge of the Li/SOCl$_2$ battery, the electrode reaction of Li/SOCl$_2$ battery is as follows:

$$Li = Li^+ + e \qquad (4)$$

$$2SOCl_2 + 4e = 4Cl^- + SO_2 + S \qquad (5)$$

In the above reaction, the Li$^+$ ions around the lithium electrode migrate to the carbon electrode surface and react with the Cl$^-$ anion:

$$Li^+ = Cl^- = LiCl \qquad (6)$$

Due to the low solubility of lithium chloride crystallite in SOCl$_2$ electrolyte, as the discharge goes on, the amount of lithium chloride crystallite deposited on the carbon electrode is increased. It can affect the electrode kinetics of the cathode discharge reaction and also causes a voltage delay owing to its overly passive nature. The different metal porphyrins as possible catalysts affect the rate of electron transfer in the above reaction.

Mechanisms of Li/SOCl$_2$ battery catalyzed by metal phthalocyanines and metal-porphyrins have been demonstrated in some papers [22, 23]. On the basis of the results and the mechanism of the catalytic reduction by metal porphyrins demonstrated by Doddapaneni and Bernstein, the possible routes are proposed to show the process of the reduction of SOCl$_2$ catalyzed by **MPp** (shown in Fig. 5). The possible routes are proposed to show the three processes of the reduction of SOCl$_2$ catalyzed by MPp and the reduction of **MPp·SOCl$_2$** is the key step: (1) SOCl$_2$ is adsorbed by **MPp**, and O atom of SOCl$_2$ coordinates to $[M]^{2+}$ of **MPp**, an adduct MPp·SOCl$_2$ is formed. (2) After that, there are different possible routes that MPp·SOCl$_2$ succeeds catalyzing the reduction of SOCl$_2$. Diverse routes showed that different numbers of electrons are accepted by **MPp·SOCl$_2$**, and **MPp·SOCl$_2$** is reduced. (3) Finally, intermediates turn into **MPp**.

The overall catalytic activity of the compounds to lithium battery depends on the competitive and cooperative reduction process of **MPp·SOCl$_2$**. With the same peripheral substituents, the three routes are primarily controlled by the electronic configuration of the central metal ions of the compounds. Among the catalysis process, the second step plays a predominant role owing to that the electron configuration of central metal. As to **Zn^{2+}Pp**, whose configuration of d electron is 3d^{10} and have the great trend to stabilize square planar of complex, so it will enhance the process of the formation of $[Zn^+Pp]^-$, S, SO$_2$ and Cl$^-$ during the reduction of **Zn^{2+}Pp·SOCl$_2$**, therefore enhancing the catalytic reaction. **Cu^{2+}Pp** also has similar catalysis. Therefore, **ZnPp** and **CuPp** exhibit excellent catalytic activity to Li/SOCl$_2$ battery. But to **Ni^{2+}Pp** and **Co^{2+}Pp**, whose d electronic configuration are 3d^8 and 3d^7, respectively and did not have enough energy to stabilize square planar of porphyrin, a series of intermediates MPp·SOCl$_2$ cannot immediately be reduced to **MPp**, **Ni^{2+}Pp** and **Co^{2+}Pp** are inoperative as a result.

SUMMARY

The influence of the electronic configuration of the central metal ion on catalytic activity of metal carboxylporphyrin to Li/SOCl$_2$ battery has been shown in this paper. The metal porphyrins with electronic configuration d^7 and d^8 of the central metal ion are inactive. The compounds **(MPp)** with electronic configuration d^9 and d^{10} of central metal ions, exhibit relatively high catalytic activity as a result of the strong trend to stabilize square planar of complexes during the reduction of **MPp·SOCl$_2$**.

Acknowledgements

This research was financially supported by the National Nature Science Foundation of China (21271148), Scientific Research Program Funded by Shaanxi Provincial Education Department (Program No. 2013JK0660), Natural Science Foundation of Shaanxi province (2013JQ2026) and Shaanxi University of Science and Technology Scientific Research Foundation for doctor (BJ11-19).

REFERENCES

1. Xu B, Zhang RL, Wang JF and Zhao JS. *J. Solid State Electrochem.* 2013; **17**: 2391–2400.
2. Zhang RL, Wang JF, Xu B, Huang XY, Xu ZW and Zhao JS. *J. Electrochem. Soc.* 2012; **159**: 704–710.
3. Barsukov IV, Gallego M and Doninger. *J. Power Sources* 2006; **153**: 288–299.
4. Ko YO and Lee CT. *J. Ind Eng. Chem.* 2012; **18**: 726–730.
5. Carmier D, Vix-Guterl C and Lahaye. *J. Carbon.* 2001; **39**: 2181–2186.
6. Carmier D, Vix-Guterl C and Lahaye. *J. Carbon*. 2001; **39**: 2187–2193.
7. Fey GT, Liu WK and Chang YC. *J. Power Sources* 2001; **97–98**: 602–605.
8. Li Y, Chen YF, Feng W, Ding F and Liu XJ. *J. Power Sources* 2011; **196**: 2246–2250.
9. Novák P, Müller K, Santhanam KSV and Haas O. *Chem. Rev.* 1997; **97**: 207–281.
10. McDonald RC and Wang WT. *J. Phys. Chem*. 1992; **96**: 9760–9764.
11. Chen M and Herzel Y. *J. Power Sources* 2004; **136**: 268–275.
12. Kim WS, Sim WJ, Chung KI, Sung YE and Choi YK. *J. Power Sources* 2002; **112**: 76–84.
13. Xu ZW, Zhao JS, Li HJ, Li KZ, Cao ZY and Lu JH. *J. Power Sources* 2009; **194**: 1081–1084.
14. Xu ZW, Zhang GX, Cao ZY, Zhao JS and Li HJ. *J. Mol. Catal. A: Chem*. 2010; **318**: 101–105.
15. Su XQ, Li J, Yao GP, Wang JL, Zhao JS and Zhang FX. *Catal. Commun*. 2013; **37**: 23–26.
16. Duan MY, Li J, Giuseppe M, Wang C and Lü XF. *J. Phys. Chem. C.* 2010; **114**: 7857–7862.
17. Petr Z, Miroslav M, Zbynek M, Kamil K and Dana S. *Dyes Pigm.* 2008; **77**: 281–287.
18. Hiroshi I, Tomokazu U and Seigo I. *Acc. Chem. Res.* 2009; **42**: 1809–1818.
19. Ma T, Kozo Inoue K and Yao K. *J. Electroanal Chem.* 2002; **537**: 31–38.
20. Lü XF, Li J, Wang C, Duan MY, Luo Y, Yao GP and Wang JL. *Appl. Surf. Sci.* 2010; **257**: 795–801.
21. Lü XF, Sun WJ, Li J, Xu WX and Zhang FX. *Spectrochim. Acta Part A*. 2013; **111**: 161–168.
22. Lee SB, Pyun SI and Lee EJ. *Elcetrochim. Acta* 2001; **47**: 855–864.
23. Wagenknecht PS and Ford PC. *J. Coord. Chem.* 2011; **255**: 591–616.